Journal of Applied Polymer Science

Zinc Oxide Nanoparticles Catalyze Rapid Hydrolysis of Poly(lactic acid) at Low Temperatures

Meng Qu, Huilin Tu, Miranda Amarante, Yi-Qiao Song, S. Sherry Zhu
Mechanics and Materials Department, Schlumberger-Doll Research, Cambridge Massachusetts 02139
Correspondence to: S. S. Zhu (E-mail: szhu5@slb.com)

ABSTRACT: Poly(lactic acid) (PLA), a biobased, degradable polymer has been used recently in the field of oil and gas. These applications require rapid hydrolytic degradation of PLA especially at low temperatures. This work reports a simple and ready-to-scale up chemistry of using zinc oxide nanoparticles (ZnO NPs) to catalyze the hydrolytic degradation of PLA at the temperatures well below its glass transition temperature. Furthermore, for the first time, we have applied the nondestructive analytical method of ^{1}H T_2 NMR relaxometry to measure the apparent rate constants of PLA hydrolysis in solid, heterogeneous/composite systems that have multiple and complex reaction kinetics. We demonstrate that the activation energy for ZnO catalyzed PLA hydrolysis is about 38% lower than that of pure PLA hydrolysis. © 2013 Wiley Periodicals, Inc. J. Appl. Polym. Sci. **2014**, *131*, 40287.

KEYWORDS: degradation; kinetics; oil and gas; biopolymers and renewable polymers; catalysts

Received 9 October 2013; accepted 11 December 2013
DOI: 10.1002/app.40287

INTRODUCTION

Poly(lactic acid) (PLA), a biobased polymer available from renewable agricultural resources, is an aliphatic polyester that degrades in water via ester hydrolysis and is also biodegradable. The degradability of PLA has been very useful for applications like drug delivery,[1,2] tissue engineering,[3] medical devices,[4] and smart materials.[5] The applications of degradable PLA have recently been extended to the oil and gas industry; for example, PLA has served as one of the important components in some fluids for hydraulic fracturing.[6,7] After fulfilling its functions in the downhole environment, PLA degrades into water soluble lactic acid. The rates of PLA degradation dramatically affect the range of its applications. The hydrolytic degradation of PLA takes a long time (months to a year) at temperatures below its glass transition temperature (T_g),[1,8–10] which excludes its applications in the low-temperature environments (<60°C). It is quite challenging to accelerate PLA degradation in neutral aqueous fluids at low temperatures.

The main interest of this research is to develop simple and ready-to-scale up chemistry to catalyze the hydrolytic degradation of PLA at the temperatures below its T_g. Zinc oxide has attracted a wide research interest because of its numerous important chemical and physical properties.[11–14] The studies of the well-defined ZnO crystals[15–20] and ZnO nanoparticles (NPs)[21,22] indicate that water partially dissociates and forms hydroxylation structures on the surfaces. The hydroxylation on ZnO surfaces affords ZnO particles some important properties, such as bonding with alkoxysilanes[23] to form polymer nanocomposites with improved thermal stability and good mechanical properties,[24,25] and anchoring polymer chains on their surfaces.[26] The acid end groups on PLA could help anchor the polymer chains on the surface of ZnO,[26] and hydroxylation of the surface of ZnO could assist the hydrolysis of PLA adsorbed on ZnO NPs (Scheme 1) by a similar mechanism reported for Al_2O_3 particles.[27,28] Despite these advantages, however, the effect of ZnO on the hydrolytic degradation of poly(α-hydroxy-esters), such as PLA, at temperatures below T_g of the polymers, is less explored.[29] To investigate the effect of ZnO NPs on the hydrolytic degradation of PLA, we incorporated ZnO NPs into amorphous PLA to form PLA/ZnO composites by a conventional melt-extrusion process, and studied their degradation in DI water at temperatures below the T_g of PLA.

We have focused on determining the rate constants of ester hydrolysis at the early stage of PLA degradation, when the molecular weight decreases without any measurable weight loss.[30–32] The traditional method to study PLA degradation at this stage is to use gel permeation chromatography (GPC) to track the change of average molecular weight or intrinsic viscosity over the time of degradation. GPC works well for pure polymers. However, for the composites/heterogeneous systems in which PLA near the surface of ZnO could have significantly

Additional Supporting Information may be found in the online version of this article.

Scheme 1. Hydroxylated ZnO NPs catalyze the rapid hydrolysis of PLA. [Color figure can be viewed in the online issue, which is available at wileyonlinelibrary.com.]

faster kinetics of hydrolysis comparing to the PLA away from ZnO NPs, the kinetics of PLA degradation derived from the GPC data may be artificially low. Thus, we chose to adapt solid-state ^1H T_2 nuclear magnetic resonance (NMR) relaxometry for more accurate measurement of the kinetics of PLA hydrolysis in these heterogeneous systems, which had not been previously used.

^1H T_2 NMR measures the proton spin-spin relaxation time, which is often used for the characterization of molecular motions.[33] Protons with different mobility inside complex material systems, such as polymers,[34,35] rocks and tissues,[36] or hydrogels,[33,37–40] present distinguishable ^1H T_2 NMR relaxation times.[35,41–44] Signal intensities of ^1H T_2 also provide valuable information of quantitative change of water protons over the time of polymer hydration.[45] Therefore, ^1H T_2 NMR relaxometry is able to measure the T_2 relaxation time and the signal amplitudes of water protons inside PLA. As the hydrolysis proceeds, the change of the signal intensity could be correlated to the change of the quantity of water molecules inside the polymer, and the rate constants of PLA hydrolysis can be derived from the rate of water consumption in a sealed system. This method is nondestructive and is especially useful to more accurately determine the degradation rate constants of solid, heterogeneous/composite systems that have multiple and complex reaction kinetics.

EXPERIMENTAL

Raw Materials

Acros organic ZnO particles, 99.5%, were purchased from Fisher Scientific, with an average particle diameter of 250 nm (BET 4.8 m^2/g). ZnO NPs, MKN-ZnO-R040, 99.9%, were purchased from MK Impex with an average particle diameter of 40 nm (BET 16.5 m^2/g). Tetrahydrofuran (THF, HPLC grade) and toluene were purchased from Sigma-Aldrich. Amorphous PLA was purchased from NatureWorks ($T_g = 57°C$).

Preparation of PLA/ZnO Composite

ZnO particles were dried in an oven at 116°C overnight. PLA pellets were ground into powder under cryogenic conditions, and oven dried at 49°C overnight; 4.1 g of PLA powders were premixed with 0.9 g of ZnO particles in a glass vial. The mixture was added into a twin-screw Thermo Haake MiniLab microcompounder as one batch. The extrusion/compounding temperature was set at 160°C and the speed of the screw was 100 RPM. The maximum torque of the extrusion was maintained below 360 Ncm. The materials were cycled inside the chamber for about 3–4 min before flushing and the total extrusion time for each batch was 6 min. The diameter of the extruded composite rod was around 2 mm. The rod was cut to 4 mm long pellets. For better comparison, pure PLA was also subjected to the same extrusion process before any degradation tests. The exact ZnO% in the resultant composites was determined by thermogravimetric analysis (TGA) using a Q500 thermogravimetric analyzer (TA Instruments). The samples were equilibrated at 40°C and then the temperature was ramped at 10°C/min to 650°C (N_2). Table I and Figure 1 show the TGA results.

Isolation of ZnO Particles from PLA/ZnO_{40} Composite

PLA/ZnO_{40} pellets (0.5 g) were dissolved in 8 mL of toluene in a glass vial. After all the pellets were dissolved to form a suspension of ZnO particles in a PLA solution, the vial containing the suspension was centrifuged at 5000 RPM for 2 h. ZnO particles settled to the bottom of the vials. The clear solution was removed using a pipet, and the ZnO particles were washed with

Table I. TGA Results of PLA and PLA/ZnO Composites

Sample	T_{D1}[a](°C)	PLA%	T_{D2}[a](°C)	PLA%$_{ZnO}$[b]	ZnO%[c]
PLA	357	99.65%			
PLA/ZnO_{40}	275	68.92%	382	11.05%	19.39%
PLA/ZnO_{40}-H[d]	251	65.35%	383	13.14%	19.79%
PLA/ZnO_{250}	291	72.27%	385	8.06%	18.82%
PLA/ZnO_{250}-H[d]	269	68.44%	383	10.28%	19.67%

[a] T_{D1} and T_{D2}: the temperatures at the maximum rate of weight loss.
[b] Percentage of weight loss at T_{D2} is the loss of PLA adsorbed on ZnO surface.
[c] Char yield at 650°C.
[d] Dried PLA/ZnO composites after hydrolyzed at 49°C for 7 days.

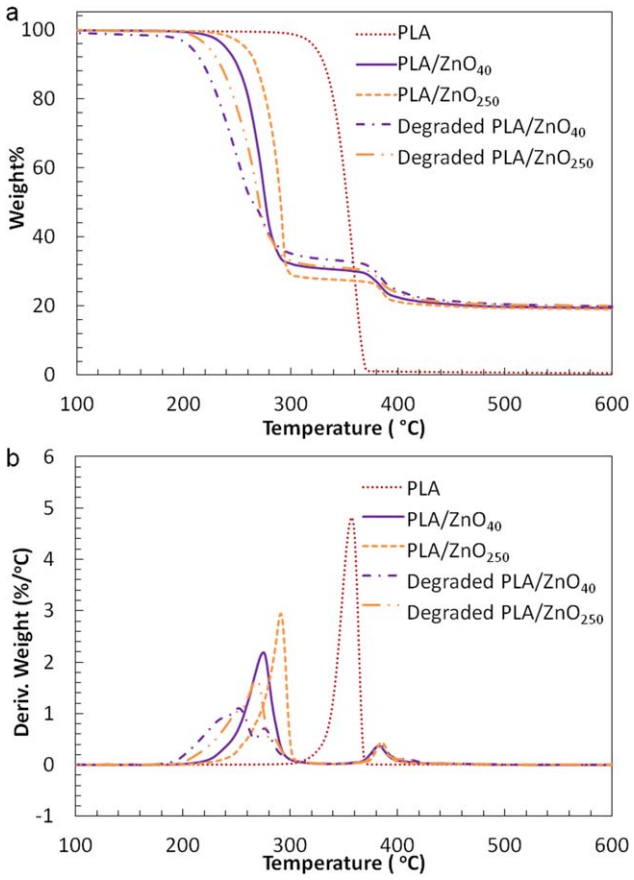

Figure 1. TGA spectra of PLA (red dotted line), PLA/ZnO_{40} (purple line), PLA/ZnO_{250} (brown dashed line), degraded PLA/ZnO_{40} (purple dashed-dotted line), and degraded PLA/ZnO_{250} (brown dashed-dotted line; after one week of hydrolysis at 49°C). (a) Weight% change vs. temperature; (b) derivative weight change vs. temperature. [Color figure can be viewed in the online issue, which is available at wileyonlinelibrary.com.]

a small amount of toluene and then centrifuged two times to remove any free PLA polymers in the toluene phase. The ZnO particles were finally washed with THF before drying in a vacuum oven at 45°C overnight to yield 0.064 g of ZnO particles (85% yield). The recovered ZnO particles were subjected to Fourier transform infrared spectroscopy (FTIR). The combined toluene solutions of the PLA polymer were extracted with 8 mL of 0.1% HCl solution to remove any ZnO particles. After separating the toluene solution from the aqueous phase, the toluene solution of PLA was added to 40 mL of methanol to precipitate PLA. The PLA precipitation was centrifuged at 5000 RPM for 2 h. The clear methanol was removed and the PLA was washed with a small amount of methanol several times and dried in a vacuum oven at 45°C overnight to yield 0.36 g of PLA (80.1% yield). The PLA was subjected to GPC to measure the intrinsic viscosity and average molecular weight.

FTIR spectroscopy with Attenuated Total Reflectance (FTIR-ATR) was conducted on the recovered ZnO particles from PLA/ZnO_{40} using a Vertex 70 (Bruker) instrument integrated with OPUS spectroscopy software and a ZnSe sample for ATR. The spectrum was scanned from 400 to 4000 cm^{-1}. For comparison, FTIR-ATR was also conducted on the pure ZnO_{40} NPs, and on the hot pressed films of the pure PLA and the PLA/ZnO_{40} composite, respectively. The results are reported in the Supporting Information.

Gel Permeation Chromatography

GPC was performed using a GPCmax VE2001 and 305 triple detector array (TDA) Detectors (Viscotek™ of Malvern). The GPCmax integrates three Styragel HR3, HR4, and HR5 columns (5 μm, 7.8 × 300 mm) from Waters Corporation. The TDA incorporates RI, Light Scattering, and Viscosity detectors. Molecular weight, size, and intrinsic viscosity of PLA were measured directly and the data was analyzed using OmniSEC software. A single narrow polystyrene (PS) calibration standard (90K from Malvern) in THF was used to calibrate the detector response and the second PS standard with a broader molecular weight distribution and a higher polydispersity was used to verify the success of the calibration. About 0.035–0.04 g of PLA polymer was dissolved in 10 mL of THF. One hundred microliters of the THF solution were injected into the GPC. THF was used as the solvent. The intrinsic viscosity was recorded for each sample.

Degradation of PLA/ZnO Composites

PLA/ZnO_{40} pellets (about 40 mg each) were kept in DI water at 49°C for 15 h to allow water to absorb into the samples. The weight change for each sample was measured before and after water exposure. The wet pellets were blotted thoroughly and quickly with Kimwipes and wrapped with Teflon film and then Parafilm. Each wrapped sample was sealed in a vial and kept at 49°C for different time intervals. One pellet was taken out of the oven each day and dried under vacuum until the weight change stopped (after about 2–3 days). The data confirm that there is no measurable weight loss after this short water exposure. The dried sample was dissolved in 10 mL of THF to remove ZnO particles by centrifuging. The clear solution was subjected to GPC measurement as described above and the polymer concentration was determined using the ZnO% in PLA (by TGA).

T_2 NMR Measurement

The samples (about 40 mg for each sample) were immersed in DI water overnight at 38, 44, or 49°C. Weight change and ^1H T_2 NMR signal were measured before and after water exposure, to quantify the amount of protons absorbed. The wet samples were blotted thoroughly with Kimwipes to remove surface water. Then, the samples were quickly wrapped with Teflon film, and placed in a NMR tube. The NMR tube was sealed with wax 8 mm from the sample to make sure that the wax is distant from the NMR transmitter/receiver coil [Supporting Information, Figure S3(a)]. The film and wax helped to prevent excessive dehydration and moisture loss during the degradation. Each sample, now in a NMR tube, was heated again in an oven at 38, 44, or 49°C, respectively, for degradation. T_2 NMR spectroscopy data was collected every 24 h from 24 to 192 h at room temperature. With this sealing method, no significant weight change of the sample was detected after testing [Supporting Information, Figure S3(b)]. The NMR relaxometry experiment uses the Carr-Purcell-Meiboom-Gill (CPMG) pulse sequence[46,47] at 400.1 MHz with an AVANCE NMR

Table II. T_2 NMR Experimental Parameters used in this Study

T_d (number of echoes)	D_1(sec)	Frequency (MHz)	90° Pulse length (μsec)	180° Pulse length (μsec)	T_e (μsec)
1024	2	400.1	10	20	50

spectrometer from Bruker BioSpin. Detailed T_2 NMR experimental parameters are listed in Table III. The number of echoes acquired (T_d) was fixed to 2048 points. A recycle delay (D_1) of 2 s was used. An echo time (T_e) of 50 μs was purposefully chosen to suppress the signal of the solid component of the polymers. That is to say, with this relatively long T_e, the T_2 signal of protons in the polymer backbone is too short to be detected. The echo decays were treated as multiexponential decays and the decay signal was analyzed using a fast Laplace Inversion algorithm[48] to obtain a spectrum as a function of T_2. With this transformation, a distribution of T_2 relaxation time was plotted versus T_2 intensity.

RESULTS AND DISCUSSION

Because the rate of hydrolysis of PLA near the ZnO NPs could be very different from the rate of hydrolysis of PLA away from ZnO NPs, we incorporate about 19% of two different sizes of ZnO NPs (e.g., ZnO_{40} and ZnO_{250}) into PLA to ensure that ZnO catalyzed hydrolysis dominates the kinetics of the PLA hydrolytic degradation, although the large amount of ZnO causes some thermal degradation of PLA during the compounding. The SEM images (Supporting Information, Figure S1) of the composites show that the NPs distribute fairly evenly despite a rather large amount being incorporated into the polymer. TGA of the PLA/ZnO_{40} composite and FTIR-ATR of the recovered ZnO particles from PLA/ZnO_{40} (treated by THF) confirm the adsorption of PLA polymers on the surface of ZnO particles. As shown in Figure 1, pure PLA has only one weight loss event at 357°C while PLA/ZnO_{40} and PLA/ZnO_{250} have their major weight loss at 275 and 291°C [D-TG, the temperature of the maximum derivative weight change, %/°C, Figure 1(b)], respectively. Additionally, TGA of both PLA/ZnO_{40} and PLA/ZnO_{250} present the second weight loss at 382–385°C, relatively insensitive to the total surface area of ZnO in the composites. This weight loss is believed to be the loss of PLA adsorbed on ZnO surfaces.[27,28] The sample of PLA/ZnO_{40} with smaller ZnO particles (larger total surface area) shows more weight loss% than that of PLA/ZnO_{250} with larger ZnO particles at 382–385°C (Figure 1). The TGA results also confirm that there is about 19% of ZnO in the composite (Table I). Moreover, the FTIR-ATR spectrum of the isolated ZnO NPs from PLA/ZnO composite shows the characteristic absorption of carbonyl stretching[49] at 1761 cm^{-1} (Supporting Information, Figure S2), which confirms the adsorption of PLA on the surfaces of ZnO.

^{1}H T_2 NMR relaxometry was conducted for PLA and PLA/ZnO samples. All the samples were immersed in DI water to allow water to absorb into the samples, and the quantitative change of water molecules inside the samples was tracked as the degradation proceeded in a sealed NMR tube (Scheme 2 and Supporting Information, Figure S3). The first challenge is to correlate the T_2 signal to the water protons. There are five possible kinds of proton motion inside PLA/ZnO composites that are detectable by the T_2 relaxation experiments: (1) rigid protons on polymer backbone that have the shortest T_2 of $10^{-6}-10^{-5}$ s (slow motion, almost static); by choosing a relatively long spin-echo time (50 μs) when using CPMG sequence,[46,47] these protons make little measurable contribution to the observed T_2; (2) side methyl groups of the amorphous PLA with some mobility that have a T_2 of $10^{-5}-10^{-4}$ s; the intensity should remain constant at constant temperatures below T_g; (3) the water protons interacting with the polymer backbone through hydrogen bonding;[50] (4) the water protons or hydroxyls interacting with the ZnO surfaces; (5) the water protons physically trapped in the pores of the polymers (but not through H-bonding). The samples were wiped clean to remove the surface water molecules that could have the longest T_2 ($\sim 10^{-1}$ s).

Figure 2 shows the ^{1}H T_2 spectra of pure PLA, ZnO_{40} NPs, and PLA/ZnO_{40} composite before and after water exposure. The small T_2 peak at 0.6 ms is the signal of the adsorbed water and hydroxyls on the surfaces of ZnO NPs (black line). The peak for the pure PLA (blue dotted line) is likely due to the residual side-chain methyl groups.[43] After water exposure, a strong T_2 peak of the absorbed water is observed at 87 μs (blue solid line). This relatively short T_2 time for the relaxation of water protons suggests strong interactions between the water molecules and the polymer backbone, likely through hydrogen-bonding.[50] After the same water exposure time, the T_2 peak of the absorbed water protons for PLA/ZnO_{40} composite (solid magenta line) is also observed at 87 μs but with higher intensity comparing to that in pure PLA. This indicates faster kinetics of water adsorption into PLA/ZnO_{40} than into pure PLA because the intensity of the T_2 peak correlates to the population of water protons inside the samples. In addition, unlike the spectrum of pure PLA, a second broad peak extending to $T_2 = 23$ ms appears on the T_2 spectrum of PLA/ZnO_{40}, indicating the presence of a different pool of water. Due to its much longer T_2 and thus much weaker interaction with the PLA or ZnO, it is likely to be the water trapped in the pores surrounding ZnO

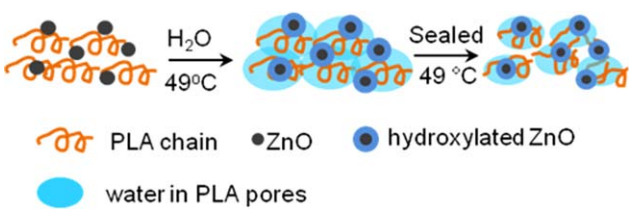

Scheme 2. Water distribution inside PLA/ZnO: before and after degradation. [Color figure can be viewed in the online issue, which is available at wileyonlinelibrary.com.]

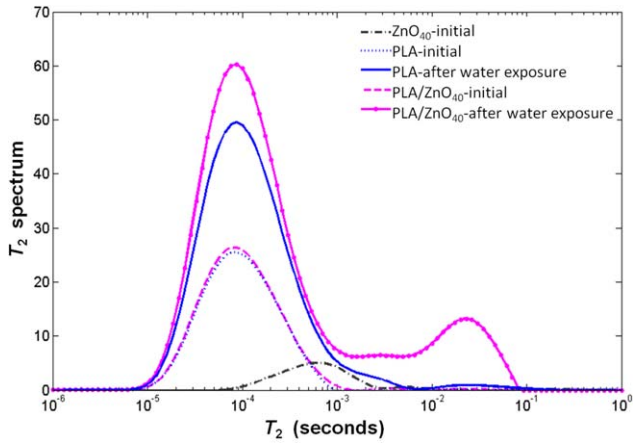

Figure 2. Comparison of the T_2 signals of PLA (blue lines) and PLA/ZnO_{40} (magenta lines) before and after water exposure. The T_2 signal of ZnO_{40} NPs is also plotted (black line). [Color figure can be viewed in the online issue, which is available at wileyonlinelibrary.com.]

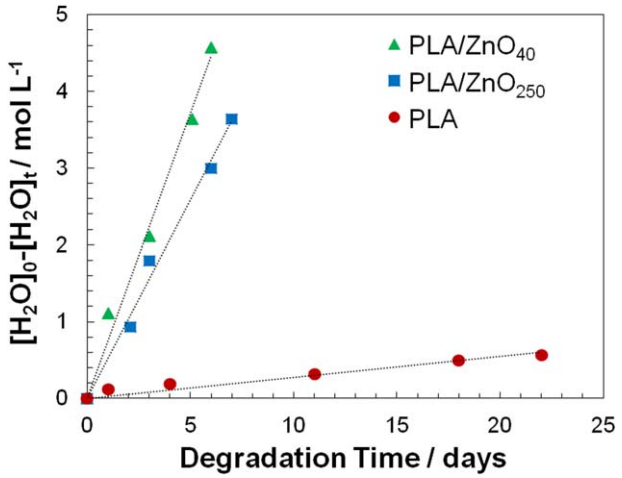

Figure 4. The zero-order kinetics of the hydrolysis of PLA, PLA/ZnO_{40}, and PLA/ZnO_{250} at 49°C. [Color figure can be viewed in the online issue, which is available at wileyonlinelibrary.com.]

NPs. The area integrations (intensity) of both ^1H T_2 peaks correlate to the amount of absorbed water, and the difference between the total intensity of ^1H T_2 peaks before and after water exposure is correlated to the moles of the total absorbed water protons (Types 3, 4, and 5), which are calculated using the weight difference of the sample before and after water exposure.

PLA degradation follows the hydrolysis of ester bonds on the polymer chain. Equation (1) describes the rate constant of ester hydrolysis:[51]

$$-\frac{d[H_2O]}{dt} = -\frac{d[\text{ester}]}{dt} = \frac{d[\text{COOH}]}{dt} = k[\text{COOR}][H_2O][\text{COOH}] \quad (1)$$

As shown in Scheme 1, hydroxides near ZnO surfaces will drive the kinetics of PLA hydrolysis. Thus, water concentration is replaced by $[OH^-]$ and is constant when the surface area of ZnO remains constant. The TGA of PLA/ZnO after their degradation indeed confirms no loss of ZnO (Figure 1 and Table I)

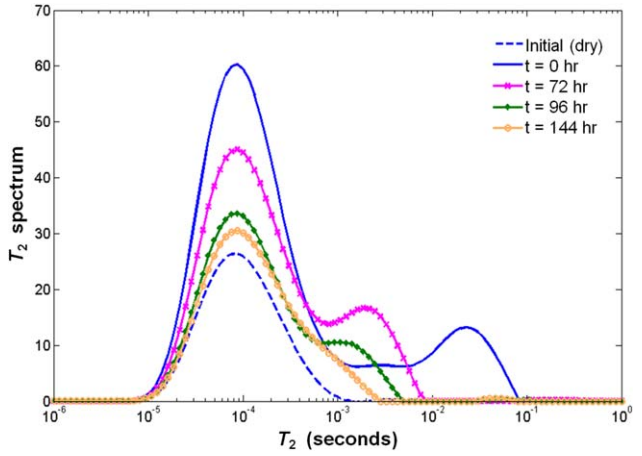

Figure 3. The changes of ^1H T_2 NMR spectrum over the time of PLA/ZnO_{40} degradation at 49°C. [Color figure can be viewed in the online issue, which is available at wileyonlinelibrary.com.]

at this early stage of PLA degradation. The ester concentration can be considered as a constant as well at this stage of degradation. The acid end groups of PLA are likely adsorbed on the surface of ZnO, and thus do not participate in the hydrolysis (no acid autocatalysis). Equation (1) is simplified to eqs. (2) and (3) that present a pseudo-zero-order rate constant k_2:

$$-\frac{d[H_2O]}{dt} = k_2 \quad (2)$$

$$[H_2O]0-[H_2O]t = k_2 t \quad (3)$$

By monitoring the quantitative change of the intensity of the ^1H (water) T_2 signals over the time of degradation of a sample sealed inside a NMR tube (Supporting Information, Figure S3), we can quantify the hydrolysis kinetics of PLA/ZnO composites.

Figure 3 shows the NMR spectra obtained on wet PLA/ZnO_{40} over degradation time up to 144 h at 49°C. The relaxation peaks of both the pore water (longer T_2) and the hydrogen-bonding water (shorter T_2,) decrease over time, indicating the consumption of water as the hydrolysis proceeds. The T_2 time of the pore water becomes shorter as well, shifting from around 23 to 1 ms over the time, suggesting that the peak is the population-weighted average T_2 of the pore water molecules that exhibit motions on more than one distinguishable time scale.[33,34,38,52] As the TGA shows that the ZnO% remains constant after the degradation (Figure 1), the down shift of T_2 as the degradation proceeds suggests that a relatively higher proportion of pore water molecules are interacting with ZnO particles when the total water population decreases (Scheme 2).

Table III. The Apparent Rate Constants of PLA Hydrolysis

	k_2 (mol L^{-1} day^{-1}) (R^2)		
Sample	49°C	44°C	38°C
PLA/ZnO_{40}	0.744 (0.99)	0.475 (0.99)	0.337 (0.95)
PLA/ZnO_{250}	0.497 (0.99)		0.254 (0.97)
PLA	0.027 (0.95)		

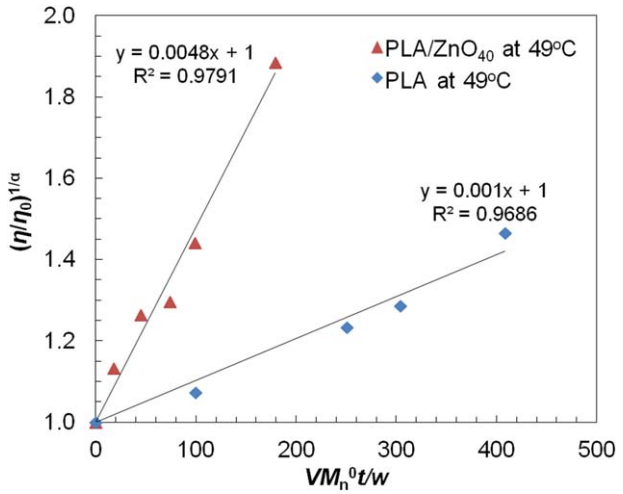

Figure 5. The rate constants, k_3, of PLA (blue) and PLA/ZnO_{40} (red) at 49°C measured by GPC. [Color figure can be viewed in the online issue, which is available at wileyonlinelibrary.com.]

The spectrum at $t = 0$ (blue solid line) represents the sample signal after exposure to DI water overnight at 49°C. The T_2 signal of the dry sample (before water exposure) is also plotted for comparison (blue dashed line). The quantitative change of absorbed water ($[H_2O]$ in mole/L) is plotted versus hydrolysis time t (eq. (3)) to obtain the zero-order rate constant k_2 at 49°C.

The same experiment was conducted for PLA/ZnO_{40} at 38 and 44°C (Supporting Information, Figure S4), for PLA/ZnO_{250} at 38 and 49°C (Supporting Information, Figure S5), and for pure PLA at 49°C. Figure 4 shows the plots of $[H_2O]_0 - [H_2O]_t$ versus hydrolysis time t at 49°C for PLA, PLA/ZnO_{40}, and PLA/ZnO_{250}. The linear fit of the plots confirms the pseudo-zero-order kinetics. The slope of each plot is the rate constant, k_2, for each sample at each hydrolysis temperature (Table II). The data shows that k_2 of PLA/ZnO_{40} is about 27 times higher than k_2 of pure PLA, and k_2 of PLA/ZnO_{250} (with smaller total surface area of ZnO) is about 30% lower than that of PLA/ZnO_{40} (Figure 4). The activation energy for the hydrolytic degradation of PLA/ZnO_{40}, calculated based on k_2 at 38, 44, and 49°C (Supporting Information, Table S1) is 59.4 kJ/mol, which is about 38% lower than that for the degradation of pure amorphous PLA (96 kJ/mol).[10] The results confirm that ZnO NPs catalyze PLA hydrolysis at temperatures well below its T_g and that the degradation kinetics are dependent on the total surface area of ZnO NPs.

For comparison, we also measured the rate constants of PLA and PLA/ZnO_{40} degradation in water at 49°C by tracking the intrinsic viscosity ($[\eta]$) change of the polymer over the time of degradation. Using the Mark-Houwink equation: $[\eta] = KM_w^{\alpha}$, and assuming the ratio of molecular distributions M_w/M_n is constant (which is confirmed by our measurement to be around 2), eq. (1) is transformed into eqs. (4) and (5) provided $[COOH] = W_s/M_nV$:

$$\frac{d[COOH]}{dt} = k_3 \tag{4}$$

$$[COOH]t - [COOH]_0 = k_3 t$$

$$\frac{M_n^0}{M_n^t} = \left(\frac{[\eta]^0}{[\eta]^t}\right)^{1/\alpha} = 1 + \frac{k_3 t}{[COOH]_0} = 1 + \frac{VM_n^0}{W_s} k_3 t \tag{5}$$

M_n^0 is the number average molecular weight of PLA or PLA/ZnO_{40} before water exposure and was calculated using the intrinsic viscosity of PLA before degradation. GPC of the pure PLA in THF determined the values K and α of the Mark-Houwink equation to be 0.00029 and 0.7, respectively. W_s is the weight of the dried sample and V is the volume of the dried sample. The ratio of intrinsic viscosity of the pellet before and after degradtion was plotted against $\frac{VM_n^0}{W_s}t$, and the slope is k_3 (Figure 5). The calculated pseudo-zero-order rate constant is 0.0048 mol $L^{-1}day^{-1}$ ($R^2 = 0.98$) for PLA/ZnO_{40} composite and 0.001 mol $L^{-1}day^{-1}$ ($R^2 = 0.97$) for pure PLA (Figure 5). This result further confirms that ZnO NPs indeed accelerate the hydrolytic degradation of PLA at temperatures below its T_g. As we expected, the difference of the rate constants between PLA/ZnO_{40} and pure PLA measured using GPC is much smaller than that derived from ^1H T_2 NMR.

CONCLUSIONS

In conclusion, PLA can adsorb on the surface of ZnO NPs. ZnO NPs function as the heterogeneous catalysts that accelerate the hydrolytic degradation of PLA in water at temperatures below its T_g. The activation energy for ZnO catalyzed PLA hydrolysis is about 38% lower than that of pure PLA hydrolysis. ^1H T_2 relaxometry is proved to be a convenient, nondestructive method for studying the early stage degradation of heterogeneous composite systems. This method can be extended to study other composite systems[53] that may have a similar catalytic effect for PLA degradation.

ACKNOWLEDGMENTS

The authors acknowledge Dr. Ravinath Viswanathan, Dr. Yucun Lou, and Dr. A. Ballard Andrews of Schlumberger-Doll Research for in-depth discussions. The authors acknowledge Center for Nanoscale Systems at Harvard for use of the SEM instruments.

REFERENCES

1. Grayson, A. C. R.; Voskerician, G.; Lynn, A.; Anderson, J. M.; Cima, M. J.; Langer, R. *J. Biomater. Sci. Polym. Ed.* **2004**, *15*, 1281.
2. Ke, C.-J.; Su, T.-Y.; Chen, H.-L.; Liu, H.-L.; Chiang, W.-L.; Chu, P.-C.; Xia, Y.; Sung, H.-W. *Angew. Chem. Int. Ed.* **2011**, *50*, 8086.
3. Lu, L.; Peter, S. J.; Lyman, M. D.; Lai, H.; Leite, S. M.; Tamada, J. A.; Vacanti, J. P.; Langer, R.; Mikos, A. G. *Biomaterials* **2000**, *21*, 1595.
4. Grayson, A. C. R.; Cima, M. J.; Langer, R. *Biomaterials* **2005**, *26*, 2137.
5. Dong, H.; Esser-Kahn, A. P.; Thakre, P. R.; Patrick, J. F.; Sottos, N. R.; White, S. R.; Moore, J. S. *Appl. Mater. Interfaces* **2012**, *4*, 503.
6. King, G. E. *SPE 152596*, Cambridge, MA 02139 USA (**2012**).

7. Willberg, D. M.; Fredd, C. N.; Bulova, M. U.S. Pat. 2011/0,056,684 A1 (**1992**).
8. Garlotta, D. *J. Polym. Environ.* **2001**, *9*, 63.
9. Codaria, F.; Lazzaria, S.; Soosa, M.; Stortia, G.; Morbidellia, M.; Moscatellib, D. *Polym. Degrad. Stab.* **2012**, *97*, 2460.
10. Zhou, Q.; Xanthos, M. *Polym. Degrad. Stab.* **2008**, *93*, 1450.
11. Wang, Z. L. *Adv. Mater.* **2012**, *24*, 4632.
12. Gomez, J. L.; Tigli, O. *J. Mater. Sci.* **2013**, *48*, 612.
13. Pearton, S. J.; Norton, D. P.; Ip, K.; Heo, Y. W.; Steiner, T. *Prog. Mater. Sci.* **2005**, *50*, 293.
14. Kurtz, M.; Strunk, J.; Hinrichsen, O.; Muhler, M.; Fink, K.; Meyer, B.; Woll, C. *Angew. Chem. Int. Ed.* **2005**, *44*, 2790.
15. Kunat, M.; Girol, S. G.; Burghaus, U.; Woll, C. *J. Phys. Chem. B* **2003**, *107*, 14350.
16. Meyer, B.; Marx, D.; Dulub, O.; Diebold, U.; Kunat, M.; Langenberg, D.; Woll, C. *Angew. Chem. Int. Ed.* **2004**, *43*, 6642.
17. Wang, Y.; Muhler, M.; Woll, C. *Phys. Chem. Chem. Phys.* **2006**, *8*, 1521.
18. Meyer, B.; Rabaab, H.; Marxa, D. *Phys. Chem. Chem. Phys.* **2006**, *8*, 1513.
19. Calzolari, A.; Catellani, A. *J. Phys. Chem. C* **2009**, *113*, 2896.
20. Onsten, A.; Stoltz, D.; Palmgren, P.; Yu, S.; Gothelid, M.; Karlsson, U. O. *J. Phys. Chem. C* **2010**, *114*, 11157.
21. Noei, H.; Qiu, H.; Wang, Y.; Loffler, E.; Woll, C.; Muhler, M. *Phys. Chem. Chem. Phys.* **2008**, *10*, 7092.
22. Raymand, D.; Duin, A. C. T. v.; W. A. Goddard, I.; Hermansson, K.; Spångberg, D. *J. Phys. Chem. C* **2011**, *115*, 8573.
23. Bussiere, P. O.; Therias, S.; Gardette, J.-L.; Murariu, M.; Duboisb, P.; Baba, M. *Phys. Chem. Chem. Phys.* **2012**, *14*, 12301.
24. Mallakpour, S.; Zeraatpisheh, F. *J. Appl. Polym. Sci.* **2012**, *126*, 1416.
25. Murariu, M.; Doumbia, A.; Bonnaud, L.; Dechief, A.-L.; Paint, Y.; Ferreira, M.; Campagne, C.; Devaux, E.; Dubois, P. *Biomacromolecules* **2011**, *12*, 1762.
26. Tang, E.; Cheng, G.; Ma, X.; Pang, X.; Zhao, Q. *Appl. Surf. Sci.* **2006**, *252*, 5227.
27. Konstadinidis, K.; Thakkar, B.; Chakraborty, A.; Potts, L. W.; Tannenbaum, R.; Tirrell, M.; Evans, J. F. *Langmuir* **1992**, *8*, 1307.
28. Tannenbaum, R.; King, S.; Lecy, J.; Tirrell, M.; Potts, L. *Langmuir* **2004**, *20*, 4507.
29. Therias, S.; Larché, J.-F; Bussière, P.-O; Gardette, J.-L; Murariu, M.; Dubois, P. *Biomacromolecules* **2012**, *13*, 3283.
30. Zhang, X.; Espiritu, M.; Bilyk, A.; Kurniawan, L. *Polym. Degrad. Stab.* **2008**, *93*, 1964.
31. Zhou, Q.; Xanthos, M. *Polym. Degrad. Stab.* **2008**, *93*, 1450.
32. Proikakis, C. S.; Mamouzelos, N. J.; Tarantili, P. A.; Andreopoulos, A. G. *Polym. Degrad. Stab.* **2006**, *91*, 614.
33. Shapiro, Y. E. *Prog. Polym. Sci.* **2011**, *36*, 1184.
34. Ibbett, R. N.; Schuster, K. C.; Fasching, M. *Polymer* **2008**, *49*, 5013.
35. Orza, R. A.; Magusin, P. C. M. M.; Litvinov, V. M.; Duin, M. v.; Michels, M. A. *J. Macromolecules* **2007**, *40*, 8999.
36. Song, Y.-Q. *J. Magn. Reson.* **2013**, *229*, 12.
37. Bline, R.; Rutar, V.; Zupancic, I.; Zidansek, A.; Lahajnar, G.; Slak, J. *Appl. Magn. Reson.* **1995**, *9*, 193.
38. McConville, P.; Pope, J. M. *Polymer* **2001**, *42*, 3559.
39. Capitani, D.; Crescenzi, V.; Angelis, A. A. D.; Segre, A. L. *Macromolecules* **2001**, *34*, 4136.
40. Diez-Pena, E.; Quijada-Garrido, I.; Spiess, H. W. *Macromol. Chem. Phys.* **2002**, *203*, 491.
41. Litvinov, V. M. *Macromolecules* **2006**, *39*, 8727.
42. Barendswaard, W.; Litvinov, V. M.; Souren, F.; Scherrenberg, R. L.; Gondard, C.; Colemonts, C. *Macromolecules* **1999**, *32*, 167.
43. McBrierty, V. D. *Polymer* **1974**, *15*, 503.
44. Ghia, P. Y.; Hill, D. J. T.; Mailletb, D.; Whittaker, A. K. *Polym. Degrad. Stab.* **1997**, *38*, 3985.
45. Wu, J.; Chen, S. *Langmuir* **2012**, *28*, 2137.
46. Carr, H. Y.; Purcell, E. M. *Phys. Rev.* **1954**, *94*, 630.
47. Meiboom, S.; Gill, D. *Rev. Sci. Instrum* **1958**, *29*, 688.
48. Song, Y.-Q.; Venkataramanan, L.; Hürlimann, M. D.; Flaum, M.; Frulla, P.; Straley, C. *J. Magn. Reson.* **2002**, *154*, 261.
49. Vey, E.; Rodger, C.; Booth, J.; Claybourn, M.; Miller, A. F.; Saiani, A. *Polym. Degrad. Stab.* **2011**, *96*, 1882.
50. Schmitt, E. A.; Flanagan, D. R.; Linhardt, R. J. *Macromolecules* **1994**, *27*, 743.
51. Pitt, C. G.; Gu, Z. W. *J. Control. Release* **1987**, *4*, 283.
52. McConville, P.; Whittaker, M. K.; Pope, J. M. *Macromolecules* **2002**, *35*, 6961.
53. Luo, Y.-B.; Wang, X.-L.; Wang, Y.-Z. *Polym. Degrad. Stab.* **2012**, *97*, 721.